MODELLING THE EFFECT OF CASING ON AFTERBURNING OF ALUMINIZED EXPLOSIVES

L. Donahue[1], R.C. Ripley[1], J. Gregson[1] and F. Zhang[2]

[1]Martec Limited, 400 - 1888 Brunswick Street, Halifax, NS, B3J 3J8, CANADA
[2]Defence Research & Development Canada – Suffield, PO Box 4000, Station Main, Medicine Hat, AB, T1A 8K6, CANADA

Previous work on cased cylindrical explosives is extended to include casing fragmentation and aluminized explosives. The objective is to determine the effect of casing expansion and fragmentation on the explosion performance of a nitromethane/aluminum slurry. For this purpose, spherical 13 μm aluminum particles are chosen to enhance the afterburning efficiency, instead of early aluminum reaction energy release to increase the work on casing wall expansion. There are several important physical phenomena that are modelled in this study including: detonation propagation through the explosive, transfer of mass, momentum and energy between the explosive and metal particles, energy release due to the reaction of particles with the detonation products and surrounding air, energy transfer to the fragmenting wall, and the confinement effect of the casing on the initial expansion, dispersal and mixing of particles with surrounding air leading to metal particle afterburning.

INTRODUCTION

Metal particles are often added to explosives to increase the energy density of the energetic material, however adding particles reduces the detonation velocity due to heat and particularly momentum transfer to the particles. The critical charge diameter for detonation failure depends on the competing effects of the explosive sensitization due to the formation of hot-spots and desensitization due to the momentum and heat transfer. Metal particles typically react after the detonation front of an explosive, where the timescales associated with particle heating and reaction time are greater and hence primarily contribute to the work done by the expanding combustion products as well as the strength and duration of the blast wave generated. Secondary combustion of the detonation products and metal particles with the surrounding air is necessary to maximize the energy release; however, under casing confinement metal particle reaction within the detonation products can help drive fragmentation.

Several researchers have performed numerical investigations into the fragmentation of cylinders filled with conventional explosives [1-3], and simplified non-ideal explosives [3]. This paper focuses on the influence of metal casing on ignition and combustion of the expanding particle cloud during explosive dispersal of a cylindrical charge filled with an aluminized explosive. For a given particle morphology and mass fraction, control of the adiabatic expansion rate of the detonation products plays a significant role in achieving this objective, and has been numerically investigated in this paper by varying casing confinement. The charges are modeled after the experiments in a previous study [4].

EXPERIMENTAL OBSERVATIONS

In addition to the critical diameter for detonation failure, a second critical diameter has been observed for explosive charges containing metallic particles: the critical charge diameter for which the particles ignite and react within the expanding detonation products (Critical Diameter for Particle Ignition or CDPI) [5]. Above the CDPI, the residence time of the particles in the hot detonation products is sufficient to overcome the quenching effect of the unsteady expansion of the products such that the particles can react. In the case of aluminum particles saturated with sensitized nitromethane in cylindrical glass tubes, the CDPI function displays a U-shaped curve for spherical particle diameters ranging from 2 – 110 μm with the minimum CDPI corresponding to an intermediate value (~54 μm) [5]. For metal casings with aluminum particles saturated in nitromethane, the CDPI was found to be a monotonic increasing function with increasing particle and charge diameter, as illustrated in Figure 1.

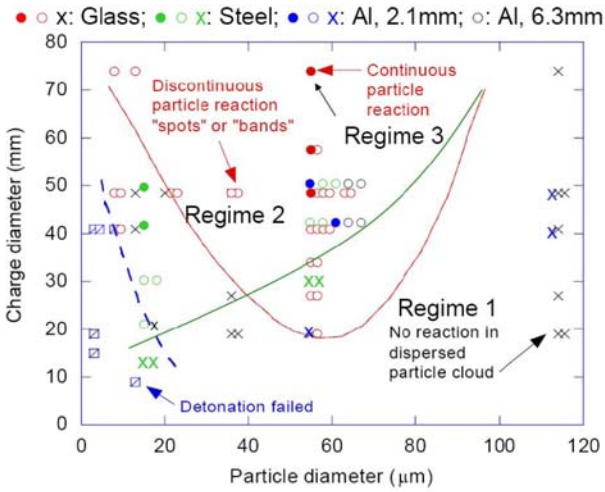

Figure 1. Dependence of particle reactivity on charge and particle diameter. Cross: Regime 1 – no reaction; Open circle: Regime 2 - reaction at isolated spots or rings; Filled circle: Regime 3 – rapid continuous reaction. [4].

The rate of convective heat transfer is a strong function of particle size and increases with a decrease in particle size. Thus, the effect of the products expansion on particle ignition and reaction becomes more sensitive for small particles, and their ignition behavior depends not only on charge diameter but also on casing confinement. For

13 μm diameter (Valimet H-10) aluminum particles, particle reaction starts for a 21 mm ID, 2.1 mm thick steel casing, while reaction of particles was observed in glass tubes only when the inner diameter was increased to 74 mm. Figure 2 shows that a rapid continuous reaction with H-10 aluminum particles took place in the expanding detonation products of a 40.1 mm ID steel-cased charge. An apparent ignition delay of about 13-18 μs was obtained by observing the reaction of the H-10 particle cloud behind the detonation front in 40.1-49.3 mm ID, 2.1 mm thick steel tubes, and it occurred mostly after the casing break-up. In the following numerical investigation, a steel tube diameter of 40.1 mm and 13 μm aluminum particles are selected to highlight particle heating, ignition and reaction at critical conditions.

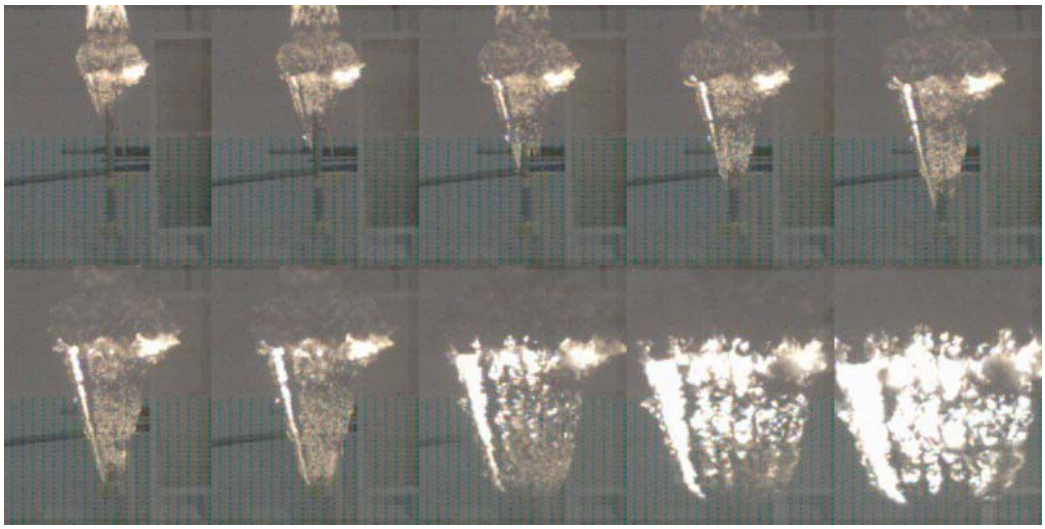

Figure 2. Detonation of nitromethane with 13 μm aluminum particles in a 1 m long, 40.1 mm ID, 2.1 mm thick steel tube, with 22.75 μs between frames and 113.75 μs for the last three frames.

NUMERICAL MODELING OF EXPLOSIVE AND CASING

The *Chinook* CFD code was used to simulate the flow features involved in the detonation of a heterogeneous cased charge including the condensed explosive, multi-component detonation products, granular material, dispersed metal particles and air. The numerical model employs a two-phase Eulerian solver and diffusion-based particle reaction model [6]. The fluid phase utilized a reaction model for the nitromethane detonation, and a JWL equation of state was used for detonation products. As air temperature is critically important to particle heating, a variable gamma ideal gas law utilizing NASA CEA thermodynamic data was employed. Tracer gases, independent of

the flow solver, were used to monitor evolution and distribution of oxidising gas species and their reaction with metal particles. Gas-particle interactions were simulated using phase exchange source terms, which are based on traditional empirical correlations for drag (momentum), heat transfer (convection) and mass transfer (particle combustion).

Chinook modelling of casing as a continuum material was performed previously in [4, 7], where the effect of casing inertia and expansion was considered in the absence of casing strength and fragmentation. To include the casing strength and allow for casing fragmentation, numerical modelling was performed using a two-way coupling fluid-structure interaction capability [8] that links Chinook and LSTC's LS-DYNA finite element code. The movement of the structural model is detected in the Eulerian CFD mesh, with pressures from the fluid being applied to the Lagrangian structural model as nodal forces. The resulting structural velocities are then applied to the fluid solution as velocity boundary conditions, and the position of the structural model is updated. Three-dimensional calculations (nominal 2 mm CFD cell size) were performed using quarter symmetry. The nodes in a uniform structural shell mesh (1 mm cell size) were shifted by random amounts, within a specific tolerance and while maintaining a constant radial distance from the centre axis, in order to artificially introduce randomness in the failure behaviour.

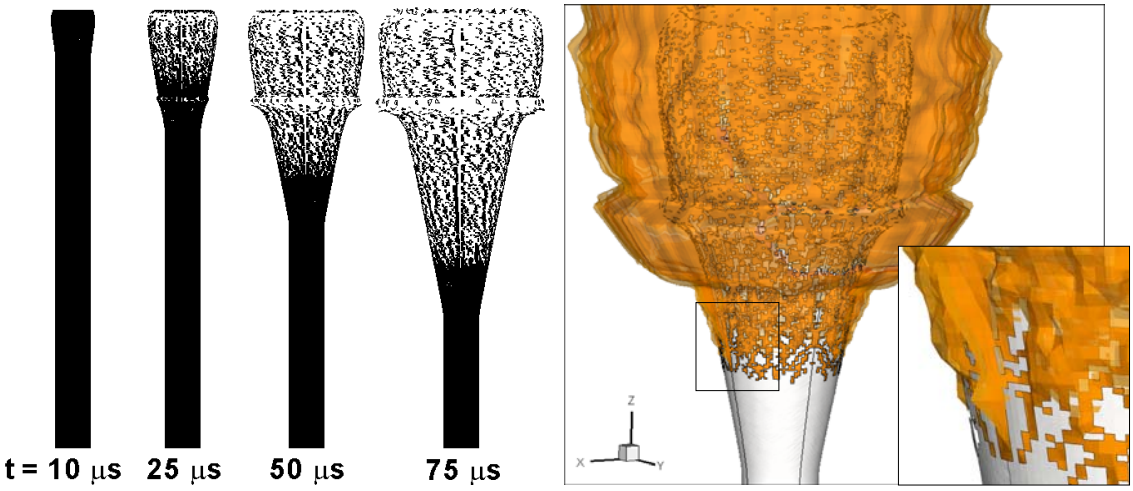

Figure 3. Chinook/LS-DYNA model of 40.1 mm ID steel cylinder. Left: Sequence of casing fragmentation for top-initiated cylindrical explosive. Right: 3D view illustrating detonation products at 50 μs. Results mirrored from quarter-symmetric model.

The detonation is initiated from the top of the cylinder along the centre axis and proceeds through the top 10 cm of booster charge consisting of sensitized nitromethane without particles. When the detonation reaches the packed particle bed, a strong shock reflection results in local high loading which causes a perturbation in the structural

failure pattern, as illustrated in Figure 3. The detonation continues through the packed particle bed, and the expanding detonation products and heated particles are accelerated through the cracks in the casing, resulting in further particle reactions with the surrounding air.

Figure 4 illustrates the dynamics of detonation of an aluminized explosive in a cylindrical casing. The curved detonation front is visible followed by a conical casing expansion over a distance of 6 cm (break-up time of 13 μs). Due to the random shell sizes employed in the 3D structural model, asymmetry is clearly evident in the solution following the casing break-up. Detonation products and metal particles with a concentration above 30 kg/m^3 have penetrated the casing fragmentation front in a chaotic, jetting fashion. Pressure contours indicate that the shock position is ahead of the dispersed particle front of 30 g/m^3 and the fragmented casing. The particle temperature in the core flow is increasing with distance from the detonation front (+y direction), however it is below the melting temperature of aluminium. Outside of the casing interface, the particle temperature increases rapidly in the shock-heated air, exceeding the melting temperature of aluminium where it is therefore presumed to react with oxidising gas species. The regions of failed casing material provide openings for local jetting of the particle front. Turbulent mixing with air outside the casing is expected to enhance particle combustion and afterburning of detonation products.

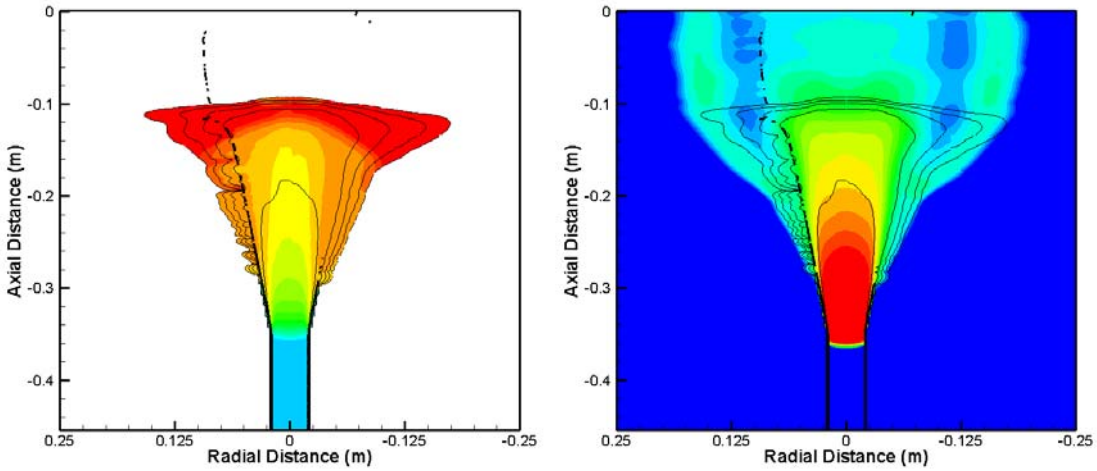

Figure 4. Dynamics of the detonation of an aluminized explosive in a cylindrical casing. Fine lines denote particle concentration ranging from 30 g/m^3 to 30 kg/m^3; Thick lines show steel casing fragments. Colour contours: (left) particle temperature from 300 to 1000 K; and, (right) gas pressure from 5 MPa to 5 GPa.

Figure 5 (left) shows the effect of confinement on the casing expansion rate and break-up time by increasing the steel wall thickness from 2.1 mm to 6.3 mm. The break-

up pattern is similar for both wall thicknesses, however the break-up time is more rapid for the thinner steel casing and therefore the dispersed particles travel farther in the radial direction. The corresponding fragment velocities following casing fracture are about 850 m/s for the 2.1 mm casing and 475 m/s for the 6.3 mm casing.

The effect of confinement on particle heating in the expanding flow was evaluated along the cylinder centreline downstream of the detonation front, with results given in Figure 5 (right). For comparison, the limiting cases of a glass cylinder (no confinement) and a rigid, non-responding casing (full confinement), are investigated. The relative confinement significantly impacts the detonation velocity and influences the particle heating rate. The particle heating rate is greatest for the fully confined configuration, due to the absence of the radial expansion of the detonation products. The particle heating rates decrease as the level of confinement is decreased. Figure 5 (right) also illustrates the expected increase in detonation velocity for the more heavily confined scenarios.

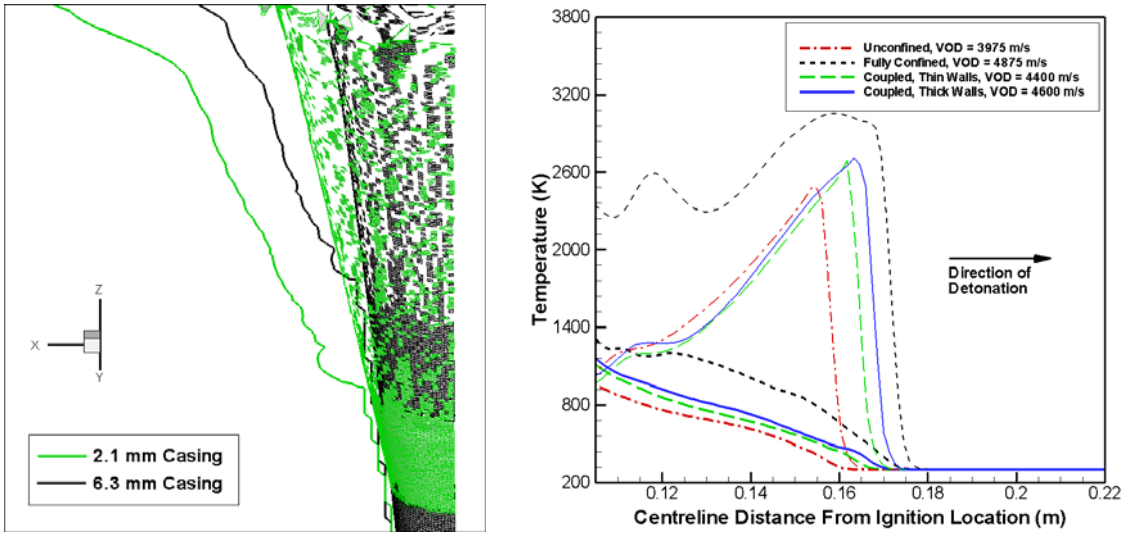

Figure 5. Effect of confinement on expansion. Left: Comparison of casing thickness on break-up and fragment velocity for steel casings at t = 75 μs; solid lines indicate position of 30 g/m^3 particle concentration. Right: Centreline particle heating rates at t = 30 μs: Thick lines give particle temperature; fine lines give fluid temperature.

To investigate the effect of particle reaction on the casing fragmentation, the particle ignition temperature was lowered such that the particles react closer to the casing break-up position, as observed in the experiments. Figure 6 shows the fluid pressures and particle temperatures along a radial slice for both levels of particle reactivity at a location 10 cm from the detonation front. Also indicated on the curves is the casing position for each result. Particle burning increases the pressures behind the

casing material, however this results in little change in casing velocity at this early time. Reacting particles increase the shock speed ahead of the casing, as well as the particle front speed.

Figure 6 (right) shows the qualitative agreement between a frame from the experimental trial and a numerical result at approximately the same time. The plots show a similar cone angle between the calculation and experiment, although at this relatively early time in the experiment, it is difficult to identify some details of the experimental response from the photographs. Experimental plots of this form are very useful for recording the actual explosive event, however data is limited to phenomena occurring on the outer surfaces of the flow. Numerical simulations allow the physics in the inner regions of the flow to be studied once a reasonable level of confidence in the models is attained.

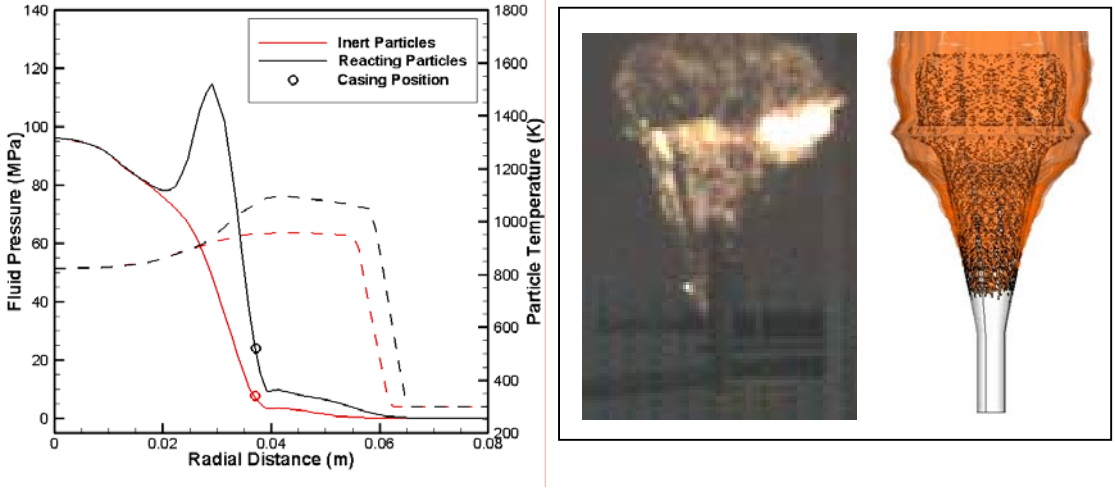

Figure 6. Left: Radial slice 10 cm behind detonation front showing effect of particle burning on expansion and casing velocity at t = 75μs. Solid lines give fluid pressure; dashed lines show particle temperature. Right: Comparison of experimental (t = 91 μs) and numerical (t = 85 μs) features.

DISCUSSION

Numerical simulations were performed to investigate the effect of casing expansion and fragmentation on the explosion performance of a nitromethane/aluminum slurry. It was determined that increasing the degree of confinement increased the particle heating rate as well as the detonation velocity. The fragmentation pattern and fragment velocities were compared for two casing thicknesses. Fragments collected from experiments are available for future comparison.

Reactive particle models are currently an area of active research. Since the particle heating model employed in the current code is based on a simple convective

heating model to illustrate the confinement effects qualitatively, the particle temperature may be underpredicted within the time that gas temperature starts to be cooled by the expansion. Mesoscale modeling of saturated metal particles [9] indicated that during the detonation interaction, mass-averaged particle temperatures reach 25-30% of the post-detonation flow temperature. Local hot spots at the particle surfaces become much hotter. Particle reflection from casing fragments may also introduce hot spots. Experiments [4] show that the reaction of the expanding 10-50 μm aluminum particle cloud occurs 10-40 μs behind the detonation front, while the reaction of the 10 μm aluminum particles in more confined detonation products takes place within microseconds. These data indicated that the oxide layers may be compromised by the detonation wave and fragmentation of the aluminum particles should not be excluded.

In the current work, only one-half of the experimental tube length was simulated. In order to make qualitative comparisons to experimental CDPI phenomenology, the simulations need to be run out further in time to eliminate the influence of detonation initiation and to reach a steady detonation and stable pattern of casing fragmentation and particle dispersal. Improved structural models that include strain-rate effects should be tested, as well as alternative methods for modelling the casing (solid elements instead of shells, different material models and failure criteria).

REFERENCES

[1] J.D. Baum, and R. Löhner, Coupled CFD/CSD modeling of a cased charge detonation and fragmentation, *18th Int. Symposium on the Military Aspects of Blast and Shock*, Calgary, Canada (2006)
[2] Q.B. Diep, J.F. Moxnes, G. Nevstad, Fragmentation of projectiles and steel rings using numerical 3D simulations, *21st International Symposium on Ballistics*, Adelaide, Australia (2004)
[3] C.K.B. Lee, Initial MAZ development I: Implementation of growing cracks on moving boundary surfaces, *18th Int. Symposium on the Military Aspects of Blast and Shock*, Calgary, Canada (2006)
[4] F. Zhang, A. Yoshinaka, D.L. Frost, R.C. Ripley, K. Kim, and W. Wilson, Casing Influence on Ignition and Reaction of Aluminum Particles in an Explosive, *13th International Detonation Symposium*, Norfolk, USA (2006)
[5] D.L. Frost, S. Goroshin, J. Levine, R.C. Ripley, and F. Zhang, Critical Conditions for Ignition of Aluminum Particles in Cylindrical Explosive Charges, *12th APS Shock Compression of Condensed Matter*, Baltimore, USA (2005)
[6] F. Zhang, D.L. Frost, P.A. Thibault, S.B. Murray, Explosive Dispersal of Solid Particles. *Shock Waves* 10: 431-443 (2001)
[7] L. Donahue and R.C. Ripley, Simulation of Cylinder Expansion Tests using an Eulerian Multiple-Material Approach, *22nd International Symposium on Ballistics*, Vancouver, Canada (2005)
[8] J. Gregson, R. Link, J.J. Lee, Coupled Simulation of the Response of Targets to Close Proximity Underwater Explosions in Two and Three Dimensions, *77th Shock and Vibration Symposium*, Monterey, USA (2006)
[9] R.C. Ripley, F. Zhang, and F.S. Lien, Detonation Interaction with Metal Particles in Explosives, *13th International Detonation Symposium*, Norfolk, USA (2006)